

Thermal Noise in Electro-Optic Devices at Cryogenic Temperatures

Sonia Mobassem^{1,2}, Nicholas J. Lambert^{1,2}, Alfredo Rueda^{1,2,3},
Johannes M. Fink³, Gerd Leuchs^{1,2,4,5},
and Harald G. L. Schwefel^{1,2}

¹The Dodd-Walls Centre for Photonic and Quantum Technologies, New Zealand

²Department of Physics, University of Otago, New Zealand

³Institute of Science and Technology Austria, Klosterneuburg, Austria

⁴Max Planck Institute for the Science of Light, Erlangen, Germany

⁵Institute of Applied Physics of the Russian Academy of Sciences, Nizhny Novgorod, Russia

E-mail: nicholas.lambert@otago.ac.nz

21 August 2020

Abstract. The quantum bits (qubit) on which superconducting quantum computers are based have energy scales corresponding to photons with GHz frequencies. The energy of photons in the gigahertz domain is too low to allow transmission through the noisy room-temperature environment, where the signal would be lost in thermal noise. Optical photons, on the other hand, have much higher energies, and signals can be detected using highly efficient single-photon detectors. Transduction from microwave to optical frequencies is therefore a potential enabling technology for quantum devices. However, in such a device the optical pump can be a source of thermal noise and thus degrade the fidelity; the similarity of input microwave state to the output optical state. In order to investigate the magnitude of this effect we model the sub-Kelvin thermal behavior of an electro-optic transducer based on a lithium niobate whispering gallery mode resonator. We find that there is an optimum power level for a continuous pump, whilst pulsed operation of the pump increases the fidelity of the conversion.

1. Introduction

Quantum computers based on superconducting qubits [1] have seen enormous progress in recent years. Quantum coherence is preserved as a consequence of reduced dissipation and the absence of thermal photons, but this typically requires cooling to below 100 mK for qubits with characteristic frequencies of ~ 10 GHz [2]. Communication between spatially separated qubits therefore presents a particular difficulty. Outside the cryogenic environment, at room temperature, the microwave frequency photons carrying the quantum information are completely swamped by thermal photons; however, visible

or near infrared photons are of much higher energy and are known to be able to carry quantum information over long distances at room temperature. Therefore, a future quantum network [3, 4] will need a method of up- and down-converting microwave photons to near infrared or visible frequency photons, to enable coherent communication between different quantum systems [5, 6, 7].

A number of approaches to microwave up-conversion have been explored [8, 9, 10, 11], using the non-linearities offered by magneto-optic materials [12, 13, 14, 15, 16], cold atom clouds [17, 18, 19, 20], quantum dots [21, 22] and opto-mechanical devices [23, 24, 25, 26]. The effect of this non-linearity is often increased by resonant enhancement of one or more of the input field, output field and optical pump. Here we focus on an electro-optic architecture [27, 28, 29, 30, 31, 32, 33], in which the required non-linearity is provided by the electro-optic tensor of lithium niobate (LiNbO_3) [34, 35]. The input field mode is defined by a metallic microwave cavity, and the output and pump by whispering gallery modes (WGMs) [36] confined to the perimeter of a LiNbO_3 disc.

The optical pump is a feature common to all up-conversion techniques, providing both the energy for the up-converted photon, and a reference frequency. The efficiency of the up-conversion process is typically improved by increasing the power in the pump, which may be as high as 1.48 mW [35], or even 6.3 mW [32] in an electro-optic realization. However, a significant fraction of the optical pump is dissipated in the device, and this can conflict with the cryogenic requirements for the environment in which superconducting qubits must be hosted. Dilution fridges, which are the usual method of attaining millikelvin temperatures, have cooling powers not significantly exceeding 1 mW [37, 38] at 100 mK with around 400 μW being more typical. Higher dissipated powers result in a dynamical thermal equilibrium with elevated temperatures. A balance exists, therefore, between choosing a pump power large enough for the up-conversion efficiency to be useful, but not so large that heating produces a high enough thermal photon population that the quality of the quantum state transfer is compromised.

The quality of the state transfer is characterized by the fidelity, which is defined as the overlap between the input and output quantum states; a fidelity of 1 corresponds to equal states (perfect conversion), and 0 to orthogonal states. Long distance quantum telecommunication [39], remote quantum state preparation [40, 41] and quantum state coherent computing [42] are often based on continuous variable (CV) states, and therefore, the fidelity between two such states lies on a continuum between 0 and 1. Examples include states of the type $|\psi_c\rangle = (|\alpha\rangle \pm |-\alpha\rangle)/\sqrt{2}$ (so-called ‘cat’ states), which are commonly used as CV-qubits [42], and squeezed states such as $|\psi_s\rangle = |\alpha, r\rangle$, which are useful in telecommunication schemes [39, 43].

Up-conversion of thermal noise to the optical channel results in a reduced fidelity of state transfer. However, so does a low conversion efficiency. In order to investigate this compromise further, we carried out thermal simulations of an efficient electro-optic modulator consisting of an optical resonator coupled to a microwave cavity [34, 44, 35]. The optical resonator is a WGM resonator made of monocrystalline LiNbO_3 , into which

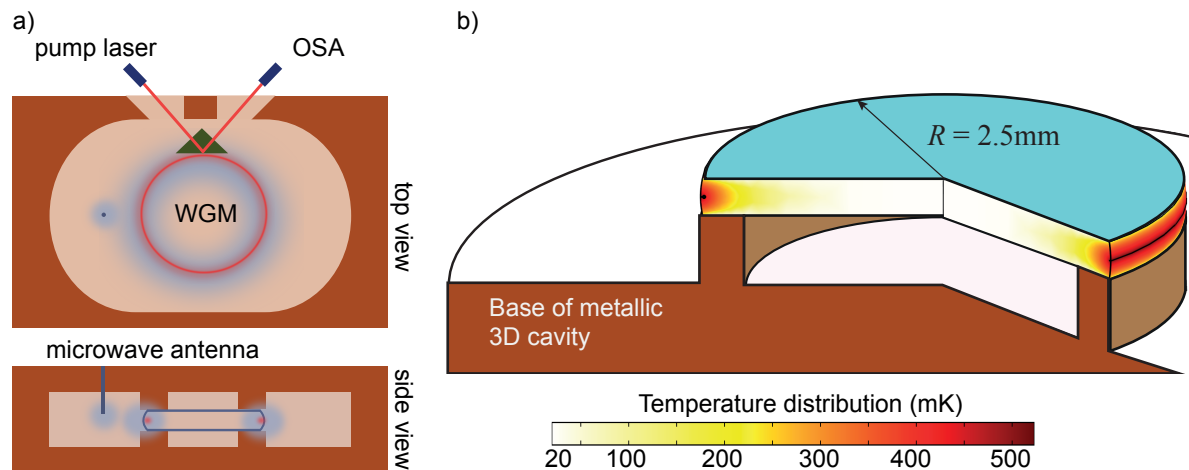


Figure 1: a) Schematic of the microwave cavity with an embedded dielectric whispering gallery mode (WGM) resonator. Light is coupled through a silicon prism and the microwave tone is inserted through an antenna. The WGM is clamped between metal rings to confine the microwave field to the optical mode volume. b) Numerical finite element simulation of the temperature distribution within the dielectric WGM assuming a critically coupled optical pump with $P_o = 1$ mW. The initial temperature of the device was $T_B = 20$ mK. The optical mode is indicated by the tiny dot close to the rim. Only one half of the metallic cavity is shown.

light is coupled using a silicon prism (see Fig. 1a). The convex geometry of the WGM resonator and transparency of LiNbO_3 confine light in the rim of the resonator via total internal reflection (see Fig. 1b). The confinement of the optical mode in a very small mode volume increases the intensity of the optical field and enhances the nonlinear interaction of light in the LiNbO_3 . The WGM resonator is embedded in a 3D copper microwave cavity, and the geometry of both resonators maximize the overlap between microwave field and optical mode.

In order to study the effect of absorption-induced heating on our electro-optic device we numerically model heat transport in a representative geometry comprising a LiNbO_3 WGM resonator with major radius $R = 2.5$ mm and side curvature $R_c = 1.45$ mm, embedded in a copper cavity (Fig. 1). The heat transfer partial differential equations are solved using COMSOL Multiphysics software, which implements a finite element method combined with a stiff ordinary differential equation solver [45, 46].

Experimental values for the thermal conductivity and heat capacity of LiNbO_3 are only available down to 4 K and for copper to around 1 K [48, 49, 47, 50]. The thermal conductivity and specific heat capacity of dielectrics such as LiNbO_3 have a T^3 dependence at cryogenic temperature. On the other hand, at very low temperatures the thermal conductivity of copper is proportional to the temperature. To estimate thermal conductivity and specific heat capacity of the materials, we make appropriate downwards extrapolations from data above 4 K, as detailed in Table 1. We neglect the thermal contact resistance at the LiNbO_3 -Cu interface, due to the smoothness of the

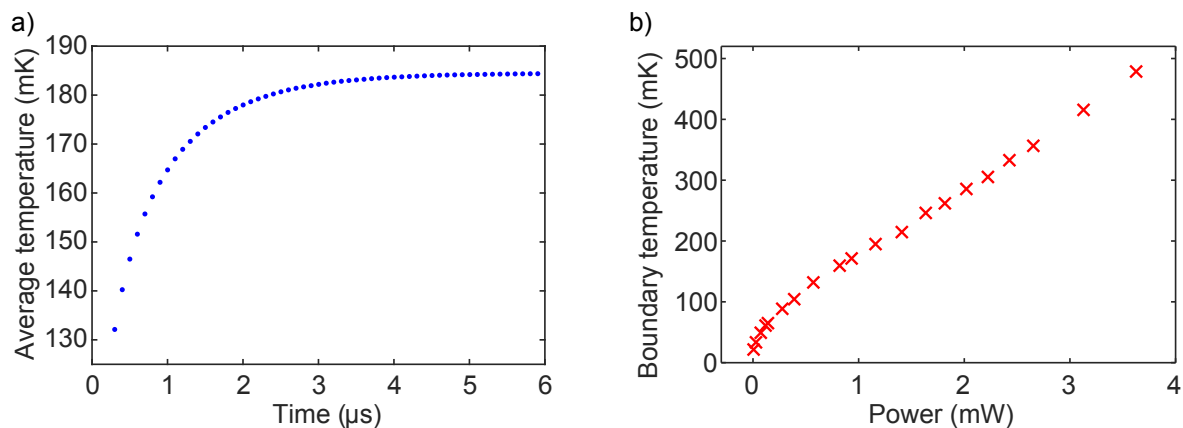


Figure 2: (a) Time evolution of average temperature of the microwave mode volume in a LiNbO_3 resonator with $200\ \mu\text{m}$ thickness and critically coupled optical pump with $P_o = 1\ \text{mW}$. Initially the cavity is at $T_B = 20\ \text{mK}$ and heats within a timescale of $3\ \mu\text{s}$ to $T_{\text{max}} = 184\ \text{mK}$. (b) Dilution fridge mixing chamber temperature (T_B) as a function of dissipated power.

LiNbO_3 and the softness of the copper generally giving a good interface, and the low thermal conductivity of the dielectric dominating heat transport (see Table 1).

In the heat transfer simulation of our microwave to optical converter, the optical pump is modelled as a heat source occupying the same volume as the optical mode. The dissipated power follows an exponential approach to the pump power P_o as $P = P_o(1 - \exp(-t/\tau))$, where τ is the rise time of optical mode (for our optical resonator $\tau \sim 1\ \mu\text{s}$, corresponding to a quality factor of $Q \sim 10^8$). The thermal boundary conditions are given by the temperature of the mixing chamber plate of the fridge. As the fridge cooling power at $T \sim 100\ \text{mK}$ is comparable to the heat load introduced by the optical pump, the boundary temperature T_B for CW operation is also a function of the power dissipated in our device. We determine typical mixing chamber temperatures for different heat loads by putting a known load on a resistive heater mounted at the mixing chamber of our BlueFors LD250, and then waiting for the temperature to stabilize (see Fig. 2(b)). The precise details of this dependency will

Table 1: Extrapolated thermal characteristics of LiNbO_3 and copper with residual resistance ratio $\text{RRR} = 100$ (thermal conductivity) and $\text{RRR} = 30$ (heat capacity) at temperatures below 1 Kelvin, assuming the functional behaviour given in Ref. [47].

	Thermal conductivity ($\text{W m}^{-1} \text{K}^{-1}$)	Heat capacity ($\text{J kg}^{-1} \text{K}^{-1}$)	Ref
LiNbO_3	$4 \cdot T^3$	$2.705 \times 10^{-4} \cdot T^3$	[48]
Cu	$500 \cdot T$	$0.01 \cdot T$	[49]

vary between cryogenic technologies and environments.

Conversely, for pulsed operation of the optical pump, the average heat load will be decreased by the duty cycle of the pump; for example, if the pump is on for only 1% of the operation cycle, then the heat load will be 1% of the pulsed power. The temperature of the cryogenic environment will then remain close to the base temperature of the fridge. To study this mode of operation, we fix our thermal boundary at $T_B = 20$ mK.

We expect the optical rise time, and therefore heating, of the device to be orders of magnitude slower than the diffusion of the heat within the dielectric. By considering the lowest order component of solutions to the heat diffusion equation, we find $t \sim \rho C d^2 / K$, with heat capacity C , thermal conductivity K and density ρ . For LiNbO₃ with a thickness of $2d = 200$ μm , the characteristic time for the heat to be redistributed is $t = 3$ ns.

The evolution of the temperature in the LiNbO₃, considering the full geometry, is calculated as a function of time, with the LiNbO₃ temperature at $t = 0$ set to the same temperature as the mixing chamber $T_B = 20$ mK. In Fig. 2(a) we plot the average temperature T_{av} of LiNbO₃ integrated over the microwave mode volume within the dielectric as a function of time for a WGM resonator thickness of 200 μm and a pump power of 1 mW. The heating occurs on a timescales of ~ 3 μs for the parameters of our cavity. We compare this calculation for the case where the optical power immediately reaches its maximum within the optical mode volume. Here the temperature saturates after only ~ 6 ns, corresponding well to the analytical toy model above.

One of the parameters affecting the time evolution of temperature is the thickness of the LiNbO₃ resonator, which is often reduced in order to increase the strength of the electric field across it. In Figs. 3(a) and 3(b) we show the saturation time and the asymptotic average temperature as a function of thickness. Since LiNbO₃ has a very low thermal conductivity compared to copper, an increase in thickness corresponds to an increase in average temperature, as well as an increase in the time taken to reach that temperature.

We now fix the thickness of the resonator at 500 μm , and study the equilibrium thermal occupancy of the microwave cavity as a function of pump power. For a mode of temperature T and angular frequency ω , the thermal photon number occupancy is

$$n = \frac{1}{\exp\left(\frac{\hbar\omega}{k_B T}\right) - 1}. \quad (1)$$

The total thermal photon number of the mode is given by

$$n_{\text{th}} = \frac{\kappa_i}{\kappa} n_{\text{th},i} + \sum_j \frac{\kappa_{e,j}}{\kappa} n_{\text{th},j}. \quad (2)$$

Here $n_{\text{th},j}$ is the thermal occupancy of the j th port of the cavity. $\kappa = \kappa_i + \sum_j \kappa_{e,j}$ is the total intensity loss rate of the cavity and is the sum of the internal loss rate, κ_i , and the loss rate via the j th port $\kappa_{e,j}$ [8]. $n_{\text{th},i}$ is the thermal occupancy of the mode due to internal fluctuations. This is directly related to internal losses by the

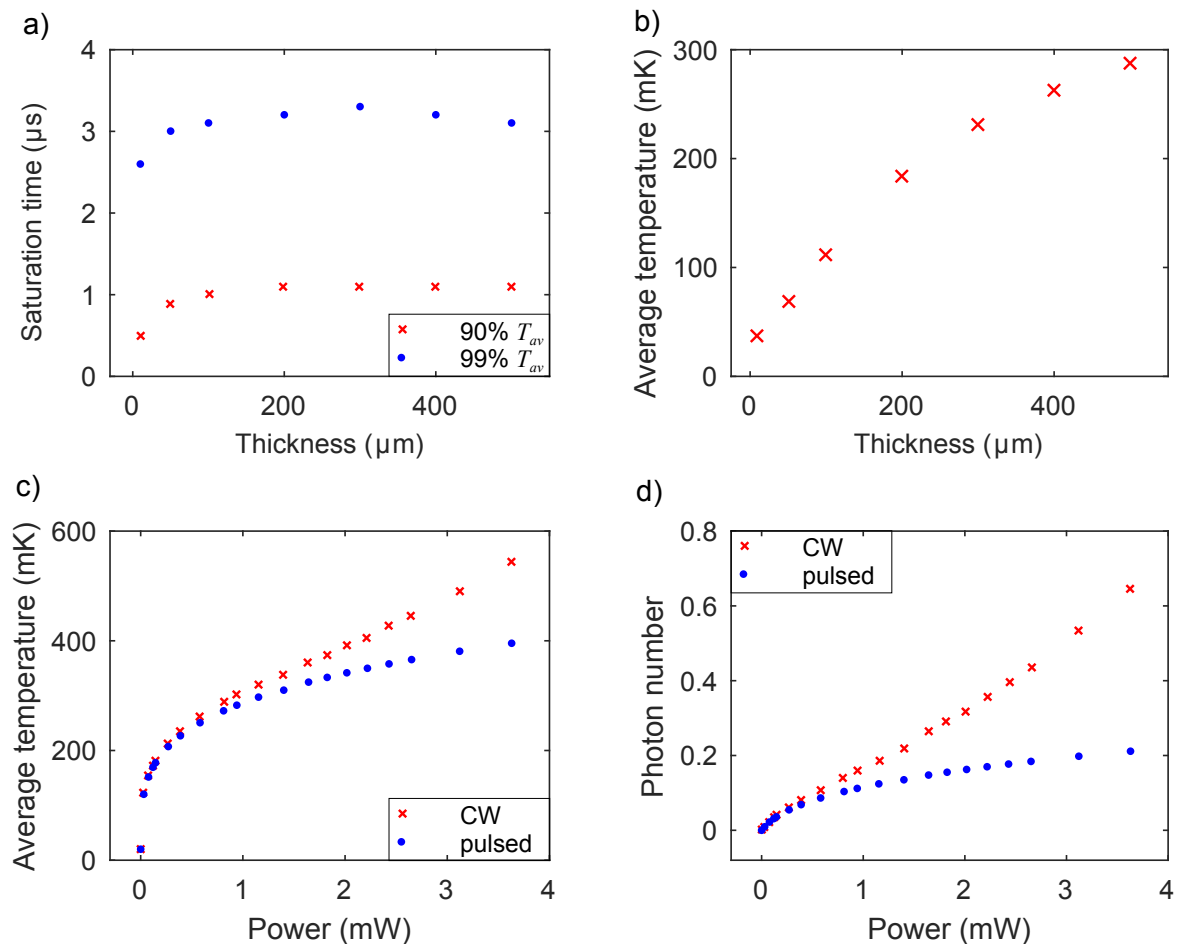


Figure 3: Numerical simulation of the optical heating of the LiNbO₃ resonator. (a) Time to reach 90% (red) and 99% (blue) of the maximum temperature integrated over the microwave mode volume within the LiNbO₃ resonator versus thicknesses of the resonator for $P_0 = 1$ mW. (b) Average equilibrium temperature of the mode volume within the LiNbO₃ resonator for different thicknesses for $P_0 = 1$ mW at $t = 0.1$ ms. (c) Average equilibrium temperature of microwave mode volume as a function of optical pump power for CW (red) and pulsed (blue) operation for 500 μm thickness at $t = 0.1$ ms. (d) Thermal photon occupancy as a function of optical pump power for CW (red) and pulsed (blue) operation for 500 μm thickness at $t = 0.1$ ms.

fluctuation-dissipation theorem [51]. Because of the large loss tangent of LiNbO₃, dielectric losses are the dominant contribution to κ_i . The microwave electric field within the LiNbO₃ is uniform, and so we use the spatial average of the temperature within the microwave mode volume inside the dielectric (Fig. 3(c)), as calculated for the asymptotic temperature distribution.

We calculate thermal photon numbers for the microwave mode of our single port cavity with angular frequency $\Omega = 2\pi \times 10$ GHz as a function of pump power, while fixing the coupling rate of the port to critical coupling ($\kappa = \kappa_i + \kappa_{e,1}$, $\kappa_i = \kappa_{e,1}$). In

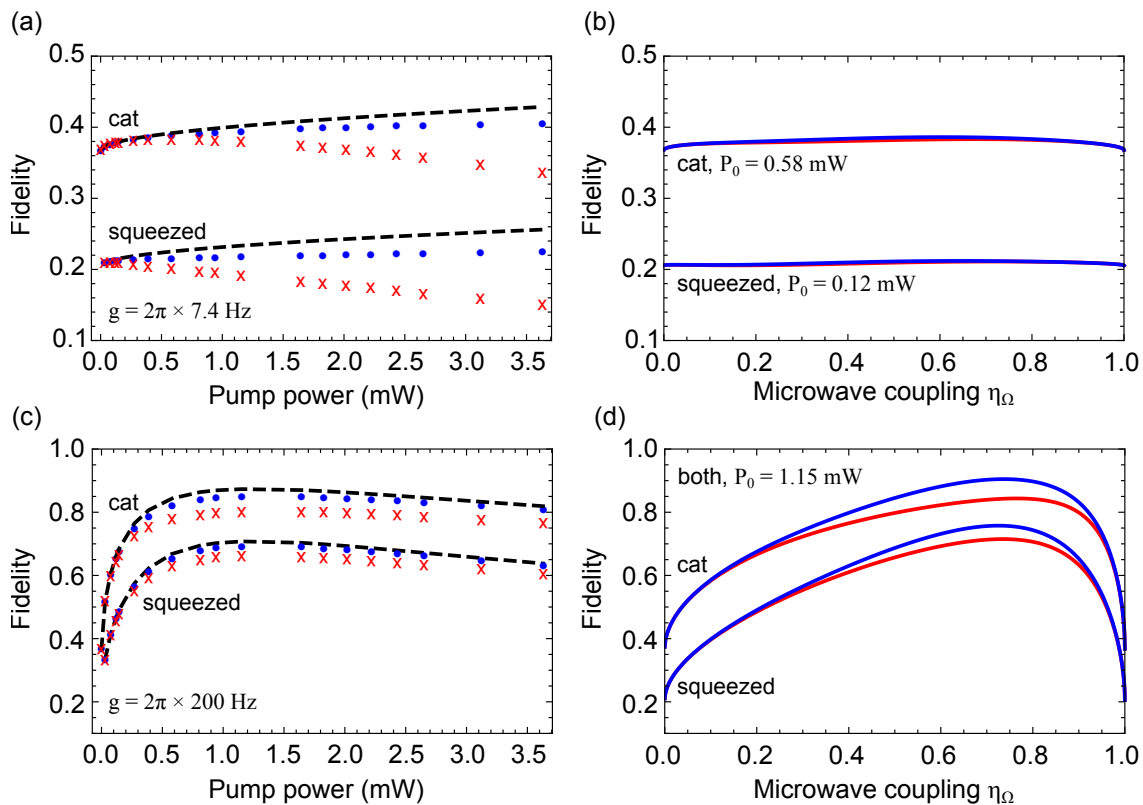


Figure 4: Dependence of fidelity on optical power and microwave coupling. (a) and (c) Fidelity versus optical pump power for cat (top) and squeezed (bottom) states for critical microwave coupling and overcoupled optical fields ($\kappa_{o,e} = 4\kappa_{o,i}$). Panel (a) is for $g = 2\pi \times 7.4$ Hz, and panel (c) for an optimised configuration with $g = 2\pi \times 200$ Hz. Results for pulsed (blue circles) and CW (red crosses) operation are shown, and dashed lines correspond to the system with no heating (where everything remains at 20 mK). (b) and (d) fidelity versus microwave coupling for optimal pump powers in panels (a) and (c). Maxima in fidelity are observed in the overcoupled regime.

Fig. 3(d) we present data for two possibilities, one in which the port temperature rises with increasing pump power due to the elevated mixing chamber temperature (CW operation of the optical pump) and one in which the port temperature remains constant at 20 mK (pulsed operation of the pump).

We calculate the effect of the simulated thermal noise on the fidelity of converted states using input–output theory from Ref. [52] for feasible experimental parameters [34]. We use the multi-photon cooperativity $C = \frac{4n_p g^2}{\kappa_o \kappa_\Omega}$, where $\kappa_o(\Omega) = \kappa_{i,o}(\Omega) + \kappa_{e,o}(\Omega)$ is the total loss rate of the optical (microwave) mode, with $\kappa_{i,o}(\Omega)$ and $\kappa_{e,o}(\Omega)$ being the intrinsic and the extrinsic damping rates of the optical (microwave) modes, respectively. We calculate the fidelity of the system while the optical resonator is critically coupled, $\kappa_{i,o} = \kappa_{e,o} = 2\pi \times 0.7$ MHz, and the microwave resonator is undercoupled, $\kappa_{e,\Omega} = 2\pi \times 7.2$ MHz and $\kappa_{i,\Omega} = 2\pi \times 32.4$ MHz. $n_p = \frac{4\eta_o P_o}{\kappa_o \hbar\omega_p}$ is the photon number corresponding to optical pump power P_o , g is the coupling strength and for our system $g = 2\pi \times 7.4$ Hz. Here,

$\eta_{\Omega(o)} = \frac{\kappa_{e,\Omega(o)}}{\kappa_{\Omega(o)}}$ is the waveguide-cavity coupling.

The fidelity of the transferred coherent squeezed state $|\alpha, r\rangle$ is given by [53]

$$F_{\text{tr}}^{\text{G}}(\alpha, r, C) = \frac{\exp\left(-2|\alpha|^2(\epsilon_3 - 1)^2\left(\frac{\cos(\phi_\alpha)}{V_-} + \frac{\sin(\phi_\alpha)}{V_+}\right)\right)}{\sqrt{\frac{\epsilon_2}{2}(1 - \epsilon_3^4) + \epsilon_3^4\left(1 + \frac{\bar{n}_\Omega(\epsilon_2 + \epsilon_2\epsilon_3^2 - 2 + \frac{\bar{n}_\Omega}{C\eta_o})}{C\eta_o}\right)}}, \quad (3)$$

where $V_\pm = 1 + \epsilon_3^2(e^{\pm 2r} - 1 + \frac{2\bar{n}_\Omega}{\eta_o C})$, $\epsilon_2 = 1 + \cosh(2r)$, $\epsilon_3 = \frac{\sqrt{4\eta_o\eta_\Omega}}{1+C}$, $|\alpha|$ is field amplitude, ϕ_α is the phase of the field, and \bar{n}_Ω is the equilibrium mean thermal photon numbers of the microwave field. The fidelity of the transferred cat state $|1\rangle - |-1\rangle$ is given by [53]

$$F_{\text{tr}}^{\text{cat}} = \frac{1}{\epsilon_4(1 + \epsilon_5)} \left[\left(1 + e^{\frac{8\alpha^2\epsilon_3}{1+\epsilon_5}}\right) e^{-\frac{2\alpha^2(1+\epsilon_3^2)^2}{1+\epsilon_5}} + 2 \cos(\phi) \left(e^{-\frac{2\alpha^2(\epsilon_3^2+\epsilon_5)}{1+\epsilon_5}} + e^{-\frac{2\alpha^2(1+\epsilon_3^2\epsilon_5)}{1+\epsilon_5}} \right) + \cos(2\phi) e^{-\frac{2\alpha^2(\epsilon_3+\epsilon_5)^2}{\epsilon_5(1+\epsilon_3)}} + e^{-\frac{2\alpha^2(\epsilon_3-\epsilon_5)^2}{\epsilon_5(1+\epsilon_5)}} \right], \quad (4)$$

where $\epsilon_4 = (1 + \cos(\phi)e^{-2\alpha^2})(1 + \cos(\phi)e^{-2\alpha^2\epsilon_3^2})$ and $\epsilon_5 = 1 + \frac{8\eta_\Gamma\bar{n}_\Omega}{(1+c)^2}$.

The fidelity for states with cooperativity $C < 1$ [34], is shown vs. the optical pump power P_o in Fig. 4(a), where the dashed lines show the noiseless case of a cat state $|1\rangle - |-1\rangle$ (top) and squeezed state $|\psi\rangle = |1, 0.5\rangle$ (bottom). The red markers indicate CW pump operation and the blue crosses pulsed operation. The maximum fidelity for CW operation is achieved at $P_o \approx 0.58$ mW for the cat state and $P_o \approx 0.12$ mW for squeezed state. Fidelities for pulsed operation are shown in blue. These do not exhibit a peak, but still diverge from the fidelities for noiseless operation as the power increases. At $P_o = 0$ the fidelity is non-zero due to the state's overlap with the vacuum.

The added noise due to dielectric heating causes a degradation of the fidelity of around 4.6% (cat state) and 4.1% (squeezed state) from the noiseless case. This problem can be reduced by over-coupling the microwave system; in this case the waveguide temperature, which is always less than the mode temperature, increases the fidelity by acting to cool the mode [35, 54, 55]. In Fig. 4(b), we fix the optical pump power to the maximum fidelity of Fig. 4(a) with $P_o \approx 0.58$ mW for the cat state and $P_o \approx 0.12$ mW for the squeezed state, and vary the microwave coupling from under-coupling ($\eta_\Omega = 0$) to over-coupling ($\eta_\Omega = 1$). For each state the red curve includes heating of the coupling waveguide (CW operation) and the blue curve describes pulsed operation which leaves the waveguide at the base temperature. We find optimal couplings for pulsed operation of $\eta_\Omega = 0.60$ (cat state) and $\eta_\Omega = 0.66$ (squeezed state), and for CW operation of $\eta_\Omega = 0.61$ (cat state) and $\eta_\Omega = 0.66$.

We now study the effects of thermal noise on an optimised transducer. The principle route to higher efficiencies in electro-optic up-convertors is by increasing the co-operativity g . In Fig. 4(c) we plot fidelity as a function of pump power for a device

with $g = 2\pi \times 200$ Hz. We find that there still exists optimal pump powers. Furthermore, in Fig. 4(d) the maximum fidelity is found to be at higher microwave overcouplings, as the cooling effect of the microwave port becomes more pronounced.

Finally, we note that in our calculations, the rise in the temperature of the copper cavity is negligible due to the relatively large heat capacity and thermal conductivity of copper, even at cryogenic temperatures. This may not be the case for superconducting cavities, in which the heat capacity is exponentially suppressed below the superconducting transition temperature. Furthermore, stray photons in a superconducting cavity may lead to a significant non-equilibrium quasiparticle population. For superconducting materials such as aluminium, an appreciable rise in the cavity material temperature may occur on longer timescales [35, 56]. Further analysis of this is beyond the scope of the present work.

In conclusion, we have demonstrated that the fidelity of quantum state transfer in electro-optic microwave-to-optical transducers is significantly affected by heating due to the absorption of the optical pump. In particular, the choice of pump power must take into account the competition between increased efficiency and increased heating that follow increased optical power. We find that, for some parameter regimes, there is an optimal power which maximises state transfer fidelity. Furthermore, there is also an optimal coupling to the microwave input waveguide which is significantly more than critical coupling. Whilst our calculations have used an electro-optic structure as an archetype, the universality of the need for an optical pump in quantum transducers means that our conclusions can be extended to other platforms. Recently optomechanical micro-devices have been demonstrated with efficient microwave-optical photon conversion [57, 58]. However, they too suffer from large thermal noise even at millikelvin temperatures when pump power is increased over a certain limit (~ 625 pW [57], ~ 40 mW [58]), showing the universal applicability of our analysis.

Acknowledgements

N.J.L. is supported by the MBIE Endeavour Fund (UOOX1805) and G.L. is by the Julius von Haast Fellowship of New Zealand. S.M. acknowledges stimulating discussions with T.M. Jensen.

References

- [1] M. H. Devoret and R. J. Schoelkopf. Superconducting Circuits for Quantum Information: An Outlook. *Science*, 339(6124):1169–1174, March 2013.
- [2] Michel H. Devoret and John M. Martinis. Implementing Qubits with Superconducting Integrated Circuits. *Quantum Information Processing*, 3(1):163–203, October 2004.
- [3] H. J. Kimble. The quantum internet. *Nature*, 453(7198):1023–1030, June 2008.
- [4] Stephanie Wehner, David Elkouss, and Ronald Hanson. Quantum internet: A vision for the road ahead. *Science*, 362(6412), October 2018. Publisher: American Association for the Advancement of Science Section: Review.

- [5] David P. DiVincenzo. The Physical Implementation of Quantum Computation. *Fortschritte der Physik*, 48(9-11):771–783, 2000.
- [6] Christoph Simon. Towards a global quantum network. *Nature Photonics*, 11(11):678–680, November 2017.
- [7] Jianming Huang and Prem Kumar. Observation of quantum frequency conversion. *Physical Review Letters*, 68(14):2153–2156, April 1992.
- [8] Nicholas J. Lambert, Alfredo Rueda, Florian Sedlmeir, and Harald G. L. Schwefel. Coherent Conversion Between Microwave and Optical Photons—An Overview of Physical Implementations. *Advanced Quantum Technologies*, 3(1):1900077, 2020.
- [9] A. A. Clerk, K. W. Lehnert, P. Bertet, J. R. Petta, and Y. Nakamura. Hybrid quantum systems with circuit quantum electrodynamics. *Nature Physics*, 16(3):257–267, March 2020.
- [10] Gershon Kurizki, Patrice Bertet, Yuimaru Kubo, Klaus Mølmer, David Petrosyan, Peter Rabl, and Jörg Schmiedmayer. Quantum technologies with hybrid systems. *Proceedings of the National Academy of Sciences*, 112(13):3866–3873, March 2015.
- [11] Nikolai Lauk, Neil Sinclair, Shabir Barzanjeh, Jacob P. Covey, Mark Saffman, Maria Spiropulu, and Christoph Simon. Perspectives on quantum transduction. *Quantum Science and Technology*, 5(2):020501, March 2020. Publisher: IOP Publishing.
- [12] Lewis A. Williamson, Yu-Hui Chen, and Jevon J. Longdell. Magneto-Optic Modulator with Unit Quantum Efficiency. *Physical Review Letters*, 113(20):203601, November 2014.
- [13] Xavier Fernandez-Gonzalvo, Yu-Hui Chen, Chunming Yin, Sven Rogge, and Jevon J. Longdell. Coherent frequency up-conversion of microwaves to the optical telecommunications band in an Er:YSO crystal. *Physical Review A*, 92(6):062313, December 2015.
- [14] Jonathan R. Everts, Matthew C. Berrington, Rose L. Ahlefeldt, and Jevon J. Longdell. Microwave to optical photon conversion via fully concentrated rare-earth-ion crystals. *Physical Review A*, 99(6):063830, June 2019.
- [15] J. A. Haigh, A. Nunnenkamp, A. J. Ramsay, and A. J. Ferguson. Triple-Resonant Brillouin Light Scattering in Magneto-Optical Cavities. *Physical Review Letters*, 117(13):133602, September 2016.
- [16] R. Hisatomi, A. Osada, Y. Tabuchi, T. Ishikawa, A. Noguchi, R. Yamazaki, K. Usami, and Y. Nakamura. Bidirectional conversion between microwave and light via ferromagnetic magnons. *Physical Review B*, 93(17):174427, May 2016.
- [17] M. Hafezi, Z. Kim, S. L. Rolston, L. A. Orozco, B. L. Lev, and J. M. Taylor. Atomic interface between microwave and optical photons. *Physical Review A*, 85(2):020302, February 2012.
- [18] Jingshan Han, Thibault Vogt, Christian Gross, Dieter Jaksch, Martin Kiffner, and Wenhui Li. Coherent Microwave-to-Optical Conversion via Six-Wave Mixing in Rydberg Atoms. *Physical Review Letters*, 120(9):093201, March 2018.
- [19] Thibault Vogt, Christian Gross, Jingshan Han, Sambit B. Pal, Mark Lam, Martin Kiffner, and Wenhui Li. Efficient microwave-to-optical conversion using Rydberg atoms. *Physical Review A*, 99(2):023832, February 2019. Publisher: American Physical Society.
- [20] A. S. Zibrov, A. B. Matsko, and M. O. Scully. Four-Wave Mixing of Optical and Microwave Fields. *Physical Review Letters*, 89(10):103601, August 2002.
- [21] Matthew T. Rakher, Lijun Ma, Oliver Slattery, Xiao Tang, and Kartik Srinivasan. Quantum transduction of telecommunications-band single photons from a quantum dot by frequency upconversion. *Nature Photonics*, 4(11):786–791, November 2010.
- [22] Anshuman Singh, Qing Li, Shunfa Liu, Ying Yu, Xiyuan Lu, Christian Schneider, Sven Höfling, John Lawall, Varun Verma, Richard Mirin, Sae Woo Nam, Jin Liu, and Kartik Srinivasan. Quantum frequency conversion of a quantum dot single-photon source on a nanophotonic chip. *Optica*, 6(5):563–569, May 2019.
- [23] R. W. Andrews, R. W. Peterson, T. P. Purdy, K. Cicak, R. W. Simmonds, C. A. Regal, and K. W. Lehnert. Bidirectional and efficient conversion between microwave and optical light. *Nature Physics*, 10(4):321–326, April 2014.

- [24] T. Bagci, A. Simonsen, S. Schmid, L. G. Villanueva, E. Zeuthen, J. Appel, J. M. Taylor, A. Sørensen, K. Usami, A. Schliesser, and E. S. Polzik. Optical detection of radio waves through a nanomechanical transducer. *Nature*, 507(7490):81–85, March 2014.
- [25] K. Stannigel, P. Rabl, A. S. Sørensen, P. Zoller, and M. D. Lukin. Optomechanical Transducers for Long-Distance Quantum Communication. *Physical Review Letters*, 105(22):220501, November 2010.
- [26] A. P. Higginbotham, P. S. Burns, M. D. Urmey, R. W. Peterson, N. S. Kampel, B. M. Brubaker, G. Smith, K. W. Lehnert, and C. A. Regal. Harnessing electro-optic correlations in an efficient mechanical converter. *Nature Physics*, 14(10):1038, October 2018.
- [27] D. V. Strekalov, H. G. L. Schwefel, A. A. Savchenkov, A. B. Matsko, L. J. Wang, and N. Yu. Microwave whispering-gallery resonator for efficient optical up-conversion. *Physical Review A*, 80(3):033810–5, 2009.
- [28] Mankei Tsang. Cavity quantum electro-optics. *Physical Review A*, 81(6):063837, June 2010.
- [29] C. Javerzac-Galy, K. Plekhanov, N. R. Bernier, L. D. Toth, A. K. Feofanov, and T. J. Kippenberg. On-chip microwave-to-optical quantum coherent converter based on a superconducting resonator coupled to an electro-optic microresonator. *Physical Review A*, 94(5):053815, November 2016.
- [30] Mohammad Soltani, Mian Zhang, Colm Ryan, Guilhem J. Ribeill, Cheng Wang, and Marko Loncar. Efficient quantum microwave-to-optical conversion using electro-optic nanophotonic coupled resonators. *Physical Review A*, 96(4):043808, October 2017.
- [31] Mian Zhang, Cheng Wang, Brandon Buscaino, Amirhassan Shams-Ansari, Joseph M. Kahn, and Marko Loncar. Electro-optic Frequency Comb Generation in Ultrahigh-Q Integrated Lithium Niobate Micro-resonators. In *2018 Conference on Lasers and Electro-Optics (CLEO)*, pages 1–2, May 2018.
- [32] Linran Fan, Chang-Ling Zou, Risheng Cheng, Xiang Guo, Xu Han, Zheng Gong, Sihao Wang, and Hong X. Tang. Superconducting cavity electro-optics: A platform for coherent photon conversion between superconducting and photonic circuits. *Science Advances*, 4(8):eaar4994, August 2018.
- [33] Jeremy D. Witmer, Timothy P. McKenna, Patricio Arrangoiz-Arriola, Raphaël Van Laer, E. Alex Wollack, Francis Lin, Alex K.-Y. Jen, Jingdong Luo, and Amir H. Safavi-Naeini. A silicon-organic hybrid platform for quantum microwave-to-optical transduction. *Quantum Science and Technology*, 5(3):034004, April 2020. Publisher: IOP Publishing.
- [34] Alfredo Rueda, Florian Sedlmeir, Michele C. Collodo, Ulrich Vogl, Birgit Stiller, Gerhard Schunk, Dmitry V. Strekalov, Christoph Marquardt, Johannes M. Fink, Oskar Painter, Gerd Leuchs, and Harald G. L. Schwefel. Efficient microwave to optical photon conversion: an electro-optical realization. *Optica*, 3(6):597, June 2016.
- [35] William Hease, Alfredo Rueda, Rishabh Sahu, Matthias Wulf, Georg Arnold, Harald G. L. Schwefel, and Johannes M. Fink. Cavity quantum electro-optics: Microwave-telecom conversion in the quantum ground state. *arXiv:2005.12763 [physics, physics:quant-ph]*, May 2020. arXiv: 2005.12763.
- [36] Dmitry V. Strekalov, Christoph Marquardt, Andrey B. Matsko, Harald G. L. Schwefel, and Gerd Leuchs. Nonlinear and quantum optics with whispering gallery resonators. *Journal of Optics*, 18(12):123002, 2016.
- [37] K. Uhlig. Dry dilution refrigerator with high cooling power. *AIP Conference Proceedings*, 985(1):1287–1291, March 2008.
- [38] XLD series dilution refrigerator. Library Catalog: bluefors.com.
- [39] S. L. Braunstein and A. K. Pati. *Quantum Information with Continuous Variables*. Springer Science & Business Media, December 2012.
- [40] J. Laurat, T. Coudreau, N. Treps, A. Maître, and C. Fabre. Conditional Preparation of a Quantum State in the Continuous Variable Regime: Generation of a sub-Poissonian State from Twin Beams. *Physical Review Letters*, 91(21):213601, November 2003.
- [41] S. Pogorzalek, K. G. Fedorov, M. Xu, A. Parra-Rodriguez, M. Sanz, M. Fischer, E. Xie, K. Inomata,

- Y. Nakamura, E. Solano, A. Marx, F. Deppe, and R. Gross. Secure quantum remote state preparation of squeezed microwave states. *Nature Communications*, 10(1):1–6, June 2019.
- [42] Jonas S. Neergaard-Nielsen, Makoto Takeuchi, Kentaro Wakui, Hiroki Takahashi, Kazuhiro Hayasaka, Masahiro Takeoka, and Masahide Sasaki. Optical Continuous-Variable Qubit. *Physical Review Letters*, 105(5):053602, July 2010.
- [43] Christian Weedbrook, Stefano Pirandola, Raúl García-Patrón, Nicolas J. Cerf, Timothy C. Ralph, Jeffrey H. Shapiro, and Seth Lloyd. Gaussian quantum information. *Reviews of Modern Physics*, 84(2):621–669, May 2012.
- [44] Alfredo Rueda, Florian Sedlmeir, Madhuri Kumari, Gerd Leuchs, and Harald G. L. Schwefel. Resonant electro-optic frequency comb. *Nature*, 568(7752):378, April 2019.
- [45] COMSOL: Multiphysics Software for Optimizing Designs.
- [46] Lennart Edsberg. *Introduction to Computation and Modeling for Differential Equations*. John Wiley & Sons, October 2015.
- [47] S. Krinner, S. Storz, P. Kurpiers, P. Magnard, J. Heinsoo, R. Keller, J. Lütolf, C. Eichler, and A. Wallraff. Engineering cryogenic setups for 100-qubit scale superconducting circuit systems. *EPJ Quantum Technology*, 6(1):1–29, December 2019.
- [48] E. Pérez-Enciso and S. Vieira. Thermal properties of intrinsically disordered LiNbO₃ crystals at low temperatures. *Physical Review B*, 57(21):13359–13362, June 1998.
- [49] P. Duthil. Material Properties at Low Temperature, January 2015. Pages: 77-95.
- [50] Adam L. Woodcraft. Recommended values for the thermal conductivity of aluminium of different purities in the cryogenic to room temperature range, and a comparison with copper. *Cryogenics*, 45(9):626–636, September 2005.
- [51] Crispin Gardiner and Peter Zoller. *Quantum Noise: A Handbook of Markovian and Non-Markovian Quantum Stochastic Methods with Applications to Quantum Optics*. Springer Science & Business Media, August 2004.
- [52] A. A. Savchenkov, V. S. Ilchenko, A. B. Matsko, and L. Maleki. Tunable filter based on whispering gallery modes. *Electronics Letters*, 39(4):389–391, February 2003.
- [53] Alfredo Rueda, William Hease, Shabir Barzanjeh, and Johannes M. Fink. Electro-optic entanglement source for microwave to telecom quantum state transfer. *npj Quantum Information*, 5(1):1–11, November 2019.
- [54] Gabriel Santamaría-Botello, Florian Sedlmeir, Alfredo Rueda, Kerlos Atia Abdalmalak, Elliott R. Brown, Gerd Leuchs, Sascha Preu, Daniel Segovia-Vargas, Dmitry V. Strekalov, Luis Enrique García Muñoz, and Harald G. L. Schwefel. Sensitivity limits of millimeter-wave photonic radiometers based on efficient electro-optic upconverters. *Optica*, 5(10):1210–1219, October 2018.
- [55] Mingrui Xu, Xu Han, Chang-Ling Zou, Wei Fu, Yuntao Xu, Changchun Zhong, Liang Jiang, and Hong X. Tang. Radiative cooling of a superconducting resonator. *Physical Review Letters*, 124(3):033602, January 2020.
- [56] Timothy P. McKenna, Jeremy D. Witmer, Rishi N. Patel, Wentao Jiang, Raphaël Van Laer, Patricio Arrangoiz-Arriola, E. Alex Wollack, Jason F. Herrmann, and Amir H. Safavi-Naeini. Cryogenic microwave-to-optical conversion using a triply-resonant lithium niobate on sapphire transducer. *arXiv:2005.00897 [physics, physics:quant-ph]*, May 2020. arXiv: 2005.00897.
- [57] G. Arnold, M. Wulf, S. Barzanjeh, E. S. Redchenko, A. Rueda, W. J. Hease, F. Hassani, and J. M. Fink. Converting microwave and telecom photons with a silicon photonic nanomechanical interface. *arXiv:2002.11628 [cond-mat, physics:quant-ph]*, February 2020. arXiv: 2002.11628.
- [58] Xu Han, Wei Fu, Changchun Zhong, Chang-Ling Zou, Yuntao Xu, Ayed Al Sayem, Mingrui Xu, Sihao Wang, Risheng Cheng, Liang Jiang, and Hong X. Tang. Cavity piezo-mechanics for superconducting-nanophotonic quantum interface. *Nature Communications*, 11(1):3237, June 2020.